Preparation and Characterization of Tungsten Trioxide (WO_3) Particles and Their Photocatalytic Performances for Methylene Blue Degradation

Lusi Ernawati[1], Ruri Agung Wahyuono[2], Inggit Kresna Maharsih[1], Ade Wahyu Yusariarta[1]
1Institut Teknologi Kalimantan
[2]Institut Teknologi Sepuluh Nopember

Keywords: Photodegradation, organic dye, methylene blue, photocatalytic, UV irradiation, WO_3

Abstract: Tungsten trioxide (WO_3) nanoparticles were successfully synthesized using sodium tungstate dihydrate ($Na_2WO_4.2H_2O$, as WO_3 source) via facile sol-gel method. This study aims to synthesize WO_3 and to investigate the effects of Na_2WO_4 precursor concentration on the particle morphology, crystallinity, and photocatalytic performance. The prepared particle can be activated under UV irradiation and showed good photocatalytic efficiency for methylene blue (MB) degradation. The results showed WO_3 dose-dependent photocatalytic performance toward 10 mg/L MB degradation. The adsorption kinetics of MB to the WO_3 catalyst surface can be evaluated and fit by using the pseudo-first-order kinetic adsorption model. The photodegradation test showed that the concentration (C_t/C_o) of 180 ml of MB decreases rapidly up to 88% with 110 mg of WO_3 for 2h irradiation.

1 INTRODUCTION

There are more than 700,000 tons of different dyes substances annually produced, among which 15% are discharged as effluent into the environment by industries such as textiles, rubber, leather, plastics, and food (Him et al., 2019). It is well known that wastewater treatment, particularly in the textile and dye industry, mainly involves the treatment of highly colored wastewater containing a variety of dyes in different concentrations. This dye-contaminated wastewater can cause harmful damage to the ecosystem and health, for example, increasing the DO (*Dissolved Oxygen*) level in the polluted ecosystem, which will result in an increase in COD (*Chemical Oxygen Demand*) (Chong et al., 2010; Coleman et al., 2007; Dai et al., 1999; Ernest et al., 2010).

There are a variety of adsorbents developed for dye removals that have been studied, among which activated carbons are most widely used. However, their current applications are limited due to their relatively high cost (Fujishima et al., 2001). Other alternative technologies are also developed for the decoloring process, for example, by coagulation techniques, flocculation, adsorption with activated carbon (Halliday et al., 2011). Nonetheless, it has been found that the color removal using these technologies only transforms the dyes from the liquid into the solid phase while they do not degrade the dye into less harmful compounds (Indonesia's Garment and Textile Sector, 2018).

Considering the limitation of the abovementioned treatment process, studies of photocatalytic degradation of organic dyes/pollutants are growing. Amongst various photocatalyst, titanium oxide (TiO_2) is considered the suitable materials for photodegradation of organic compounds as it is inexpensive, largely available, thermally stable, and harmless [9]. However, this material has a relatively wide energy bandgap (Eg) of 3.2 eV, which limits further applications of the material in the visible-light region (λ + 390 nm) (Ke et al., 2018). In this regard, tungsten trioxide (WO_3) has been proposed as an attractive candidate due to its high stability in aqueous solution under acidic conditions. Furthermore, its low energy bandgap (Eg) of 2.4-2.8 eV (Kang et al., 2001) allows for a photocatalytic process triggered under visible solar spectrum (Kim et al., 2006) and the conduction band level of WO_3 is suitable to allow favorable charge transfer to

Ernawati, L., Wahyuono, R., Maharsih, I. and Yusariarta, A.
Preparation and Characterization of Tungsten Trioxide (WO3) Particles and Their Photocatalytic Performances for Methylene Blue Degradation.
DOI: 10.5220/0009193000050011
In *Proceedings of the 1st International Conference on Industrial Technology (ICONIT 2019)*, pages 5-11
ISBN: 978-989-758-434-3

generate intermediates OH• responsible for pollutant degradation (Michalow et al., 2009).

While the preparation of WO_3 nanoparticles is often reported using complicated synthetic routes that require high-temperature process, pressure, and expensive apparatus (Kang et al., 2001; Kim et al., 2006; Michalow et al., 2009), the work at hand presents a facile way and low-cost approach to synthesize WO_3 nanoparticle *via* sol-gel method at mild temperature. The crystallite morphology and structure are discussed upon varying the ratio between precursor and surfactant. The dose-dependent of WO_3, as well as the dye concentration-dependent to photocatalytic activities for the Methylene Blue (MB) degradation, are studied in detail.

2 EXPERIMENTAL METHODS

2.1 Synthesis of WO_3 Particles

The synthesis was conducted through acidic precipitation method using $Na_2WO_4.2H_2O$ under mild condition. An amount of $Na_2WO_4.2H_2O$ was dissolved in 50 ml of aqua dest and stirred for 30 min. Subsequently, 2 M of HCl was added into the solution to reach pH < 6 and heated up to 90ºC. Afterward, the CTABr solution was poured into the mixture (with 1 :1, 2 :1, and 4 :1 ratio to $Na_2WO_4.2H_2O$), and white precipitation was formed. The mixture solution was kept at 90ºC and stirred for another 30 min. Finally, the precipitates were filtered, dried in an oven (100ºC, 1 h), and annealed in the furnace at 500ºC for 4 h.

2.2 Photocatalytic Performance of WO_3 Particle for Methylene Blue Degradation

Photocatalytic activity of WO_3 against organic pollutants, i.e., methylene blue (MB), was assessed. MB photodegradation tests were carried out employing a different dose of WO_3 catalysts and different concentrations of MB. The photocatalyst was soaked in the aqueous MB solution and then transferred into a custom-built photoreactor and irradiated under UV light (T5-UV7-W, 254 nm in wavelength) for several times, i.e., every 15 min for 2 h. The solution was stirred to increase contact between photocatalyst and MB molecules. In addition, the reactor was isolated from the ambient light irradiation. Photodegradation of MB was detected through absorption change at 665 nm measured using a UV/vis spectrometer (Rayleigh UV-9200). The decrease of MB optical density was used to determine the decreasing MB concentration due to the catalytic activity of the WO_3 catalyst.

2.3 Characterization

X-Ray Diffraction (XRD) patterns were obtained using a PAN analytical type X'Pert Pro diffractometer with Cu-Kα as the radiation source operated at 40 kV and 40 mA. Samples were scanned between 10 and 100° diffraction angle (2θ) with a resolution of 0.05°. Crystallite size was estimated using the Debye-Scherrer equation. SEM image of WO3 powder was measured by scanning electron microscopy (SEM, FEI type Inspect 21) at 100 kV accelerating voltage. Fourier-transform infrared (FTIR) spectroscopy was carried out using PerkinElmer Spectrum version 10.5.1.

3 RESULTS AND DISCUSSIONS

3.1 Physical and Microstructural Properties of WO3 Particle

SEM micrographs (Figure 1) showed the morphology of the resultant WO_3 particles by the different concentration of sodium tungstate, including 0.1; 0.2 and 0.3 M after annealing at 500ºC for 4 h. The morphology of synthesized WO_3 particles exhibits a small spherical shape. Nonetheless, WO_3 particles show particle size distribution with a high polydispersity for all molar ratio used in this work, Na_2WO_4 (0.1 M, Dp= 42.16) ; Na_2WO_4 (0.2 M, Dp= 55.27) ; and Na_2WO_4 (0.3 M, Dp= 47.72). Hence, the results indicate that the concentrations of Na2WO4 play an insignificant rôle to tune the particle size. In addition, aggregation is observed as a small WO_3 particle tends to be unstable and easier to form aggregates than larger particles (Szekely et al., 2016). The aggregation is also plausibly formed due to interactions and collisions between particles (Morales, 2008).

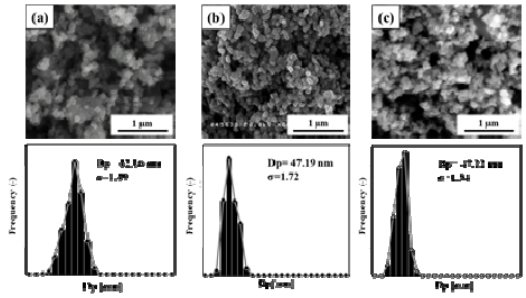

Figure 1. Morphology of synthesized WO3 particle with variation of Na2WO4 concentration (a) 0.1 M, (b) 0.2 M and (c) 0.3 M.

The microstructures of prepared WO_3 particles were characterized by XRD analysis. The results are shown in Figure 2.

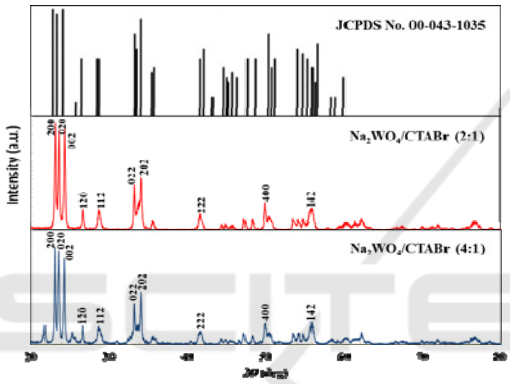

Figure 2. XRD powder diffractogram of WO_3 with variations composition of Na_2WO_4 / CTABr.

According to JCPDS (No. 00-043-1035), the prepared WO3 shows characteristic of a monoclinic WO3 crystal structure indicated by diffraction angle 2Θ at 23.15°, 23.66°, 24.37°, 26.63°, 28.76°, 33.30°, 34.16°, 41.71°, 49.96°, and 55.93°. The crystallite size is then estimated using the Scherrer equation (Table 1).

Table 1. The crystallinity of WO_3 particles with different composition of Na2WO4/CTABr

WO_3 Sample	**Crystal Size (nm)**	**Crystallinity (%)**
Na_2WO_4/CTABr **(2:1)**	40,39	89,33
Na_2WO_4/CTABr **(4:1)**	45.68	90,01

The crystallinity of synthesized WO_3 particle, as shown in Table 1 also does not show a significant difference, i.e., the crystallinity is found as high as 90%. It should be noted that the crystallinity is influenced by the calcination temperature. The higher the calcination temperature of WO_3, the higher the crystallinity (Palupi, 2006). The crystallite size of WO_3 using Na_2WO_4/CTABr (4:1) is larger than WO_3 Na_2WO_4/CTABr (2:1). It is indicating that CTABr, as a surfactant, is able to prevent collisions among WO_3 particles during nucleation leading to a slower formation of WO_3 particles as well as the nucleation rate. Therefore, the size of the WO_3 particles is getting smaller with respect to the higher concentration of CTABr (Papp, 1994).

3.2 FTIR Spectra of WO3 Particle

The functional groups of WO_3 particles were characterized by FTIR, as shown in Figure 3. The IR spectra exhibit distinct peaks between 400 and 4000 cm^{-1}. Both WO3 particles show a peak at 3304.06 cm^{-1}, which assigned to the vibration of O-H bonds of water content in WO_3 (Patel and Vashi, 2015). Notably, WO_3 particle with the composition of Na2WO4/CTABr (2:1) shows the OH group vibration at 1622.13 cm-1 and 1408.04 cm-1 (Petsom et al., 2018). In addition, both WO3 particles exhibit IR peaks at 1039.63 cm-1 that can be ascribed to W-OH bond vibration (Sanchez-Martinez et al., 2014). Further IR fingerprint of W-O bonds is characterized by peaks within the range of 500-1000 cm^{-1}.

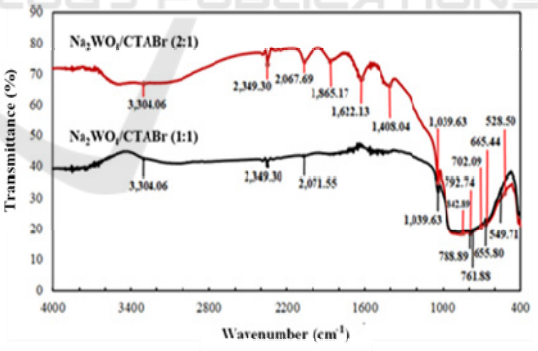

Figure 3. FTIR spectra of WO_3 Compounds with the varied composition of Na_2WO_4 / CTABr.

Comparing these two particles, WO_3 prepared using Na_2WO_4 / CTABr (2:1) shows a strong vibration at 842.89, 792.74, 702.09, 665.44, and 528.50 cm^{-1}. Meanwhile, WO_3 prepared using Na_2WO_4 / CTABr (1:1) exhibit slightly different strong vibration bands at 788.89, 761.88, 655.80, and 549.71. All of these bands can be indicative of a W-O-W bond (Szekely et al., 2016). Thus, it can be deduced that pristine WO_3 particles (without impurities) are obtained.

3.3 Effect of WO_3 amount on MB Degradation

The initial investigation of photocatalytic activity is carried out to understand the effect of the WO_3 dose on the photocatalytic degradation of MB as organic pollutants. The photoreactor containing 10 ppm of MB solution and the amount of WO_3 particles tested is varied by 70 mg, 90 mg, 110 mg, and 150 mg. The photographs of MB degradation with variations amount of WO_3 is depicted in Figure 4. Upon the pictorial view, 70 mg of WO_3 cannot fully degrade the MB after 120 minutes' irradiation. However, the colorless solution is observed upon using at least 90 mg WO_3 catalyst after 120 minutes irradiation. In addition, maximum degradation is obtained using 150 mg of WO_3.

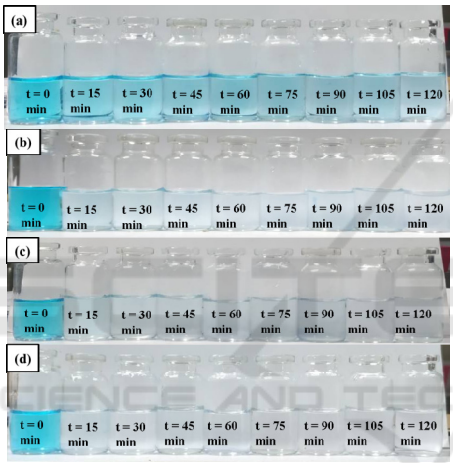

Figure 4. Photographes of MB degradation at 120 minutes using variation amount of WO_3 particle (a) 70, (b) 90, (c) 110, and (d) 150 mg.

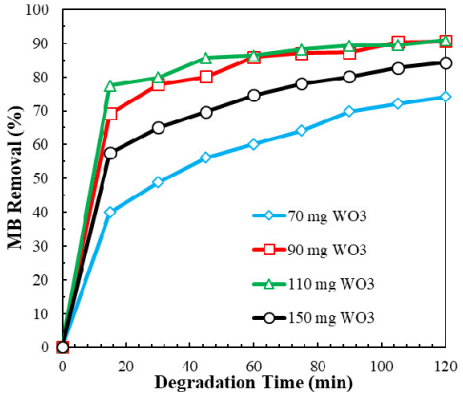

Figure 5 The time-dependent MB concentration using different amounts of WO_3 particle. The amount of MB (10 ppm) was kept constant.

The quantitative results of MB degradation by WO_3 particle are shown in Figure 5. It is shown that at least 70% of MB is degraded using 70 mg of the catalyst after irradiation. The photocatalytic activity tends to be low at a minimum dose of 70 mg (39.89% degradation) at 15 minutes, while the high and rapid photocatalytic activity is obtained using 150 mg, i.e., 95.8% MB is degraded within 15 minutes. Overall, the results show that the rate of MB degradation depends on the dose of the WO_3 catalyst. The higher concentration of catalyst used will increase MB percentage removal because the surface area of the catalyst increases. The increased surface area influences the number of existing active sites and the magnitude of the reaction rate of the photo-generated electron-hole pairs on the surface to react with water creating more oxidant agents, which increases the efficiency of photocatalytic activity (Wang et al., 2019).

It is interesting to note that 110 mg and 150 mg dose of catalyst do not show significant difference since the available active sites provided using 110 mg are already sufficient (reach a saturated value) to adsorb the amount of MB in solution. The stagnant and even decreasing degradation upon increasing the dose of catalyst can also be caused by increasing turbidity. Increasing the turbidity of the solution decreases the absorption of light, which related by the number of particles capable of capturing photons and producing reactive oxidants to degrade organic compounds (Werth et al., 2003).

3.4 Effect of MB Concentration

Further investigation is carried out to understand the effect of MB concentration on the photocatalytic degradation process. In this regard, the photoreactor containing 10 mg mL-1 of WO_3 particles was used, and the concentration of MB solution tested was varied by 5, 10, 15, and 20 mg L-1. The qualitative results are indicated in Figure 6, while the quantitative results are shown in Figure 7.

It is apparent that the concentration of MB as a coloring agent affects the photocatalytic activity (Figure 7). The concentration of MB at 5 mg L^{-1} has the largest MB removal, which reaches 100% while at 10 mg L^{-1} MB is the smallest MB removal (88.7%). For 20 mg L^{-1} concentration is MB removal marked by 90%, while 94% MB removal is obtained for 15 mg L^{-1} concentration. The results obtained above can be explained as follow: The less concentrated MB solution (5 mg L^{-1}) can increase the degradation rate because the oxidants OH• produced by the reaction between catalysts and

specific H_2O and H_2O_2 are able to degrade all MB in 75 minutes. However, in this study, the smallest % MB removal is owned by the MB concentration of 10 mg L^{-1}, which can be due to randomly limited MB adsorption on the surface of the catalyst and diffusion at the active site of the catalyst (Wicaksana et al., 2014). When the MB concentration is sufficiently high, more MB can be adsorbed and diffused at the active site of the catalyst. As a result, more OH• are generated and able to efficiently degrade MB on the surface catalyst (Zheng et al., 2011).

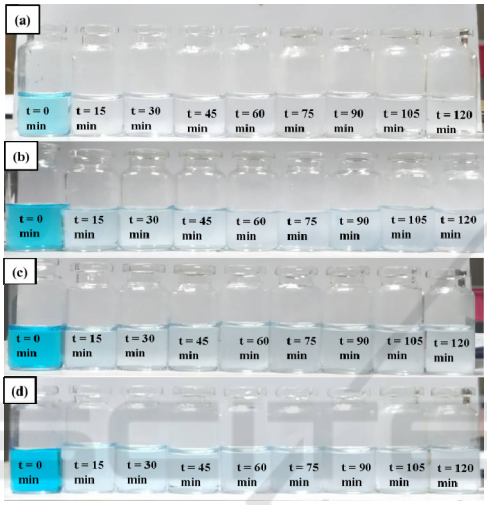

Figure 6. Photographes of MB degradation after 120 minutes' irradiation using variation concentration of MB (a)5 mg/L, (b) 10 mg/L, (c) 15 mg/L, (d) 20 mg/L.

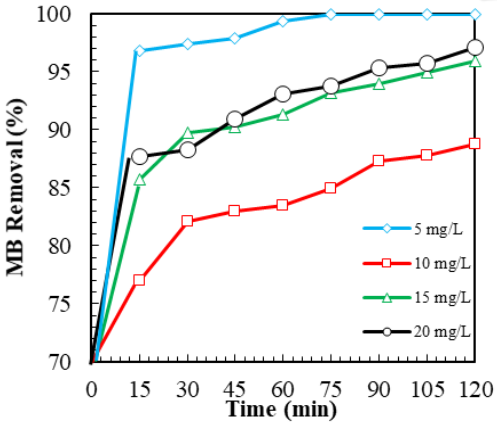

Figure 7 The corresponding percentage of MB degradation under various MB concentration. The amount of WO_3 (110 mg) and stirred at 300 rpm.

In this study, the reaction rate constant (K) is approached and determined using the homogeneous system following first-order reaction (n =1). Kinetics of photodegradation using different amount of WO_3 catalyst is therefore evaluated following *pseudo-first-order kinetic* expression:

$$r = \frac{-dC}{dt} = K.C^n \qquad (3)$$

Where K is the reaction rate constant, and n is the order of the reaction. The order of reaction and reaction rate constants are determined from the integration of the reaction rate equation resulting in a linear equation, in which K is the slope of the linear curve.

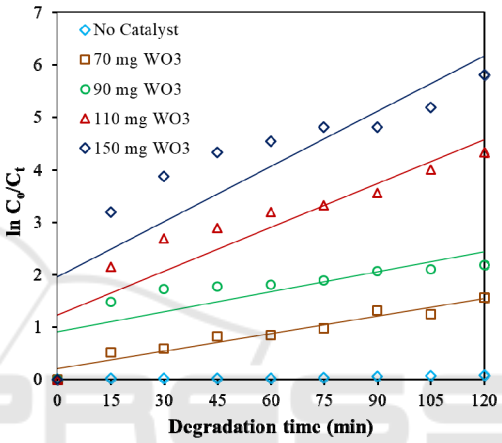

Figure 8. Time-dependent ln (Co/Ct) for photodegradation of MB (10 mg L^{-1}) under different amount of WO_3 particles (70, 90, 100, and 150 mg).

Table 2. Reaction rate constants (K) and the coefficient of determination (R_2) obtained for photodegradation of MB using different amount of WO_3

WO_3 amount	k (min^{-1})	R_2
No Catalyst	k1 = 0.0006	0.9073
70 mg	k2 = 0.0111	0.9383
90 mg	k3 = 0.0127	0.6198
110 mg	k4 = 0.0279	0.8097
150 mg	k5 = 0.0351	0.7227

The kinetic study reveals that pseudo-first-order reaction is sufficient to fit the kinetic data. Hence, it can be understood that the MB molecules are physisorbed on the catalyst surface prior to exposing the photocatalytic process. The kinetic study also indicates that the increasing amount of WO_3 induces the rate of reaction to increase as indicated by the increasing slope at a higher amount of WO_3. It is apparent that the amount of WO_3 influences the rate of the reaction (Table 2). The catalyst amount of 150 mg has the highest reaction rate (0.0351 min^{-1}),

while the catalyst amount of 90 mg has the lowest reaction rate (0.0111 min^{-1}). The results obtained here show promising performance as compared to the reaction rate obtained for other WO_3 nanostructures reported in the literature (Zheng et al., 2011; Ernawati et al., 2019).

4 CONCLUSIONS

WO_3 nanoparticles were successfully synthesized by acidic precipitation-assisted sol-gel method using $Na_2WO_4.2H_2O$ as a precursor and CTABr as a reactive agent. It is found that the composition of CTABr and $Na_2WO_4.2H_2O$ during the synthesis affects the aggregation formation of WO_3 nanoparticles. However, varying composition does not yield a significant difference in the crystallinity of nanoparticles. The photocatalytic degradation test of MB in aqueous medium indicates a WO_3 dose-dependent performance as well as MB concentration-dependent performance. The kinetic study unravels that the initial mechanism of MB degradation using WO_3 is physisorbtion of the dye molecules on catalyst surface as indicated by the pseudo first-order kinetic fit. The highest reaction rate constants were obtained by using 150 mg of WO_3 catalyst (k5 = 0.0351 min^{-1}).

ACKNOWLEDGMENT

The author would like to thank Laboratorium Pusat Sentral Material Maju dan Terbarukan (Universitas Negeri Malang) for technical assistant of material characterizations. This research is supported by Lembaga Penelitian dan Pengabdian Masyarakat (LPPM) Institut Teknologi Kalimantan, Indonesia.

REFERENCES

Chi Him, A. T., Kai, L., Yuxuan, Z., Wei, Z., Tao, Z., Yujie, Z., Ruijie, X., Dennis, Y. C. L., Haibao, H. 2019. Titanium oxide Based photocatalytric materials development and their role for the air pollutant degradation: overview and forecast. 125, 200-228.

Chong, M. N., Jin, B, Chow, C. W, Saint, C., 2010. Recent developments in photocatalytic water treatment technology: A review. Water Res 44:2997–3027.

Coleman, H. M., Vimonses, V., Leslie, G., Amal, R., 2007. Degradation of 1,4-dioxane in water using TiO_2 based photocatalytic and H_2O_2/UV processes. *J. Hazard Material*, 146, 496-501.

Dai, Q., Zhang, Z. He, N., Li, P. Yuan, C., 1999. Preparation and Characterization of Mesostructured Titanium Dioxide and Its Application as a Photocatalyst for the Wastewater Treatment. *J. Materials Science and Enginering*. 8-9, 417-423.

Ernest M.H., Tanapon P., Gregory V. L., 2010. Nanoparticle Aggregation: Challenges to Understanding Transport and Reactivity in the Environment. J. Quality, 39, 1909-1924, Carnegie Mellon University, Qatar.

Fujishima, A., Rao, T. N., Tryk, D. A., 2001. Titanium dioxide Photocatalysis. *J. Photocem and Photobio*, 1, 1- 21.

Halliday, D., Resnick, R., Walker, J., 2011. *Fundamentals of Physics.* Hoboken, N. J. Wiley.

Indonesia's Garment and Textile Sector, 2018. Remain Optimistic Amid Mounting Pressure. Global Business Guide Indonesia.

J. J. Moses., L. Ammayappan., 2015. Growth of textile industry and their issues on environment with reference to wool industry.

Ke, D., Liu, H., Peng, T., Liu, X., 2008. Preparation and photocatalytic activityof WO_3/TiO_2 nanocomposite particles. *J. Materials Letters*, 62, 447-450.

Kang, Y. S., Myun, K. P., Young, T. K., Hyun, W. L., Won, J. C., Wan, I. L., 2001. Preparation of Transparent Particulate MoO_3/TiO_2 and WO_3/TiO_2 Films and Their Photocatalytic Properties. *J. Catalyst*. 191, 192-199.

Kim, J. O., Traore, M. K., Warfield, C., 2006. The textile and apparel Industry in Developing Countries. *Textile Progress*, 38(3), 1-64.

Michalow, K. A., Heel, A., Vital, A., Amberg, M., Fortunato, G., Kowalski, K., Graule, T.J., Rekas, M., 2009. Effect of Thermal Treatment on the Photocatalytic activity in Visible Light of TiO_2-W flame Spray Synthesized Nanopowders., Top. Catal. 52, 1051-1059.

Morales, W., 2008. Combustion Synthesis and Characterization of Nanocrystalline WO_3. The University of Texas at Arlington, Arlington.

Palupi, E., 2006. Degradasi Methylene Blue dengan Metode Fotokatalisis dan fotoelektrokalasis menggunakan film TiO_2. Skripsi. Institut Teknologi Bandung.

Papp, J., Soled, S., Dwight, K., Wold, A., 1994. Surface Acidity and Photocatalytic Activity of TiO_2, WO_3/TiO_2 and MoO_3/TiO_2 Photocatalysts. *Chem. Mater.* 6, 496-500.

Patel, H., Vashi, R. T., 2015. Characterization and treatment of textile wastewater. Elsevier: 3 -5.

Petsom, K., Kopwitthaya, A., Horphathum, M., Ruangtaweep, Y., Sangwarantee, N., Kaewkhao, J., 2018. Shape-controlled synthesis of tungsten oxide nanostructures and characterization. *J. Metals, Materials and Minerals,* 28, 69-75.

Sanchez-Martinez, D., Hernandez-Uresti, D. B., Cruz, A. M. L., Guzman-Sepulveda, S., Torrez-Martinez, L. M., 2014. Characterization and Photocatalytic properties of hexagonal and monoclinic WO_3 prepared

via microwave-assisted hydrothermal synthesis. J. Ceramics, 40:4767-4775.

Szekely, I., Kovacs, G., Baja, L., Danciu, V., Pap. Z., 2016. Synthesis of shape-tailored WO_3 micro/nanocrystals and the photocatalytic activity of WO_3/TiO_2 composites. *J. Materials*, 9(258), 1-14.

Wang, W. W., Fu, H. T., Yang, X. H., An, X. Z., 2019. Preparation and visible-light-driven photocatalytic activity of WO_3/TiO_2 core-shell nanorods, *International Workshop on Materials Science and Mechanical Engineering*, 504.

Werth J.H., M. Linsenbuhler, S.M. Dammer, Z. Farkas, H. Hinrichsen, K.-E Wirth, dan D.E. Wolf., 2003. Agglomeration of Charged in Nanopowder Suspensions, Germany.

Wicaksana, Y., Liu, S., Scott, J., Amal, R., 2014. Tungsten Trioxide as a Visible Light Photocatalyst for Volatice Organic Carbon Removal. *J. Molecules*, 19, 17747-17762.

Zheng, H., Ou, J.Z., Strano, M.S., Kaner, R.B., Mitchell, A., Kalanta-zadeh, K., 2011. Nanostructured Tungsten Oxide-Properties, Synthesis, and Applications. *Adv.Funct. Mater*. 21(12), 2175–2196.

Ernawati, L., Wahyuono, R. A., Muhammad, A. A., Nurislam Sutanto, A. R., Maharsih, I. K., Widiastuti, N., Widiyandari, H., 2019. Mesoporous WO_3/TiO_2 Nanocomposites Photocatalyst for Rapid Degradation of Methylene Blue in Aqueous Medium. *International Journal of Engineering TRANSACTION A: Basics*, 32, 1345-1352.